# Design optimisation of $CO_2$ gas cooler/condenser in a refrigeration system

Y.T. Ge[*],  S.A. Tassou , I  Dewa Santosa   K. Tsamos

RCUK National Centre for Sustainable Energy Use in Food Chains (CSEF)

School of Engineering and Design, Brunel University

Uxbridge, Middlesex, UB8 3PH, UK

**Abstract**

As a natural working fluid, $CO_2$ has been widely applied in refrigeration systems where heat is conventionally released to ambient through external airflow. Owing to its extraordinary thermophysical properties, especially a low critical temperature, the $CO_2$ heat release through a high-pressure side heat exchanger will inevitably undergo either supercritical or subcritical processes, depending on ambient air temperatures and head pressure controls. Correspondingly, the heat exchanger will act intermittently as either a gas cooler or condenser within the system during an annual operation. Such evidence should therefore be taken into account for an optimal design of the heat exchanger and head pressure controls in order to significantly enhance the performance of both components and the associated system.

To achieve these targets, two $CO_2$ finned-tube gas coolers/condensers with different structural designs and controls have been purposely built, instrumented and connected with an existing test rig of a $CO_2$ booster refrigeration system. Consequently, the performance of the $CO_2$ gas coolers/condensers with different structure designs, controls and system integration at different operating conditions can be thoroughly investigated through experimentation. In the meantime, models of the finned-tube $CO_2$ gas coolers/condensers have been developed using both the distributed (detailed model) and lumped (simple model)

methods. The former is employed to give a detailed prediction of the working fluid temperature profiles, localized heat transfer rates and effects of pipe circuitry arrangements, while the latter is suitable for the simulation and optimisation of system integration with less computation time. Both models have been validated with measurements, and moreover the simple model has been integrated with other component models so as to create a system model. The effects of the $CO_2$ gas cooler/condenser sizes and controls on the system performance can thus be compared and analysed.

*Keywords: $CO_2$ gas cooler or condenser; test facilities; experiment and modelling; heat exchanger sizes and controls; refrigeration system*

\* Corresponding author. Tel.: +44 1895 266722; fax: +44 1895 256392.
E-mail address: Yunting.Ge@brunel.ac.uk (Y.T. Ge).

**Nomenclature**

| | | | |
|---|---|---|---|
| $A$ | heat transfer area (m$^2$) | *Subscripts* | |
| $C_{pa}$ | constant pressure specific heat of air (J/kg.K) | *a* | *air* |
| $Gc$ | heat flow rate (W/K) | *aflow* | *air flow* |
| $h$ | enthalpy(J/kg) | *ain* | *air inlet* |
| $\dot{m}$ | *mass flow rate* (kg/s) | *air_on* | *air on* |
| *Mrin* | refrigerant inlet mass flow rate (kg/s) | *aout* | *air outlet* |
| *NTU* | Number of Transfer Unit | *f* | *fin* |
| $P$ | pressure (pa) | *i* | *inner* |
| *Prin* | refrigerant inlet pressure (bar) | *in* | *inlet* |
| $\dot{Q}$ | heat transfer rate (W) | *is* | *isentropic* |
| $R$ | ratio | *max* | *maximum* |
| $T$ | temperature (°C) | *min* | *minimum* |

| | | | |
|---|---|---|---|
| *tamb* | ambient air temperature (℃) | *r* | *refrigerant* |
| trin | refrigerant inlet temperature (℃) | *rin* | *refrigerant inlet* |
| *U* | heat transfer coefficient (W/m$^2$.K) | *o* | *outer* |
| *UA* | overall heat conductance (W/K) | *out* | *outlet* |
| $\dot{V}$ | volumetric flow rate (l/s) | *p* | *pressure* |
| $\alpha$ | heat transfer coefficient (W/m$^2$.K) | tot | total |
| $\varepsilon$ | heat transfer effectiveness (-) | | |
| $\eta$ | efficiency(-) | | |
| $\rho$ | density(kg/m$^3$) | | |

## 1. Introduction

As an environmentally friendly working fluid with superb thermophysical properties, $CO_2$ has been readily applied in refrigeration and heat pump systems. Air cooled finned-tube condensers used in conventional refrigeration systems have also been greatly exploited in $CO_2$ systems with cascade arrangements or all-$CO_2$ transcritical arrangements [1-3] of which the $CO_2$ heat exchangers operate as either condensers or gas coolers, depending on ambient conditions and 'head' pressure controls. Therefore, it is demonstrable that due to the low critical temperature and very high critical pressure of the $CO_2$ fluid, a $CO_2$ refrigeration system can periodically operate between high performance subcritical cycles and less efficient transcritical cycles. However, this operating efficiency can be significantly improved through the use of an expansion turbine, a liquid-line/suction-line heat exchanger (llsl-hx), and more efficient system equipment such as a compressor, evaporator or gas

cooler/condenser [4], as well as optimal controls of refrigerant high-side pressures [5]. The feasibilities of such strategies can be substantiated through system experiment and modelling.

An experimental investigation was carried out on a two-stage $CO_2$ transcritical refrigeration system with external intercooling [6]. In the test rig, air-cooled finned tube gas coolers with different structures and circuits were installed in the high pressure side. The test results showed that an optimal head pressure did exist to maximize the system COP which was necessarily controlled in actual operations. Alternatively, it would be beneficial for a direct staging $CO_2$ transcritical system such as the $CO_2$ booster refrigeration system to be studied experimentally. To understand the performance of a $CO_2$ air cooled gas cooler, a series of tests were conducted at different operating conditions using a purposely designed test facility [7]. The effects of air and refrigerant side flow parameters on the heat exchanger heat transfer and hydraulic behaviours were examined. In addition, the temperature profiles along the heat exchanger circuit pipes were measured. Further investigation, including a model development, will be implemented to predict these effects on the performance of the associated system. Apart from the overall performance investigations of the $CO_2$ gas coolers, the in-tube cooling processes of $CO_2$ supercritical flow were extensively tested and correlated [8-10], which is helpful for the model development of a $CO_2$ gas cooler.

In terms of the theoretical analysis of $CO_2$ gas coolers, two modelling methods can be used, ε-NTU or LMTD i.e. lumped method and distributed method [11,12]. The lumped method is simpler, requires less computation time and is thus suitable for simulating a complex system with an integrated heat exchanger. However, such a modelling method can only provide a reasonable prediction accuracy if appropriate correlations are applied [13]. The rapid change of $CO_2$ thermophysical properties with temperature during an isobaric gas cooling process means that it is not practical to use ε-NTU or LMTD method to simulate gas coolers if detailed information of refrigerant temperature profile and localised heat transfer

rate along circuit pipes are required, or if the performance effect of different pipe circuit arrangements are to be examined. The detailed model, however, will take a much longer computation time especially when it involves a whole-system simulation [14]. Although the performances of $CO_2$ finned-tube gas coolers or condensers have been investigated extensively using both experimental and theoretical methods, research on the effect of their integration with associated systems is still rather limited [15]. To some extent, this could lead to inaccurate design and mismatching of the heat exchanger size and control when applied to a real system. The combined analysis of the heat exchanger can also contribute towards the selection and design of other matched components and appropriate system controls.

In this paper, the performance of the $CO_2$ gas cooler or condenser has been investigated experimentally in a purposely-built $CO_2$ gas cooler test rig, which is connected to a $CO_2$ transcritical booster refrigeration test facility. Models of the finned-tube $CO_2$ gas cooler and condenser have been developed using both lumped and distributed methods which have been validated against test results. The simple (lumped) model was then integrated with other component models to establish an overall system model. The effect of heat exchanger sizes and pipe circuitry arrangements on system performance and controls at different operating states has been investigated.

## 2. Experimental Facilities

To examine experimentally the performance of $CO_2$ gas coolers or condensers with different sizes and operating conditions, a test rig has been purposely built, as shown in Fig. 1. The $CO_2$ heat exchanger is suspended tightly between two upright metal frames. A propeller air fan with variable speed control is installed above the heat exchanger to maintain

a fixed airflow. Above it are a number of smaller air fans installed in opposition along the direction of pipe length that will switch on if the air on temperature is controlled to be higher than ambient. As such, part of the hot exhaust air will flow back through the return air tunnels, then return air grills, and mix with lower temperature ambient air flow. If the mixed air flow temperature is still lower than the designed air on temperature, an electric air heater installed just beneath the heat exchanger will be switched on to maintain the air on temperature. Consequently, the gas cooler air on parameters, temperature and flow rate, can be well controlled to specified values. The test rig has been comprehensively instrumented to detailed measurement data and overall performance description of the heat exchanger itself and its integrated $CO_2$ refrigeration system. These include two thermocouple meshes with 24 points each to measure air-on and air-off temperatures; pressure difference of air flow through the heat exchanger to ascertain the air side pressure drop, average air flow velocity to obtain the air flow rate. To get a more accurate average air flow velocity, a number of points crossing the heat exchanger air on surface are measured and averaged. For the refrigerant side, four pressure transducers are installed inside the inlet and outlet headers and one circuit of the heat exchanger to measure the overall and heat exchanger refrigerant side pressure drops. In addition, as shown in Fig. 2, a large number of thermocouples are attached on all the pipe bends along the pipes of one circuit to measure refrigerant temperature variation or profile from inlet to outlet. Instead of measuring the refrigerant mass flow rate directly, it is calculated from the heat exchanger heat balance between the air and refrigerant sides. The tested heat transfer rate is calculated as equation (2) in section 3 based on the measurements in the air side. Such a rate is set to be balanced by the heat transfer rate calculated by equation (1) in section 3.

The tested gas cooler/condenser is connected with its integrated refrigeration system, as depicted in Fig. 3; this allows it to pass through the refrigerant flow at a constant flow rate

within specific superheated parameters. The refrigeration layout is actually part of a $CO_2$ booster system in which the tested gas cooler/condenser is connected to two parallel high-temperature compressors and a liquid receiver. In the refrigeration system, there are three pressure levels: high, intermedium and medium, which are controlled respectively by the back pressure valve (ICMT) connected after the gas cooler, bypass valve (ICM) and thermostatic expansion valve (AKV-MT). The approach temperatures at the gas cooler and condenser outlets are controlled by the gas cooler fan speed and ICMT while the system cooling capacity is modulated with variable speeds of compressors. In Fig. 3, at one test condition, sample measured parameters of temperatures and pressures at each component inlet and outlet are also indicated.

All the sensors in the system were calibrated before the experiments to ensure acceptable accuracy with thermocouples uncertainty less than $\pm 0.5$ $^0$C, pressure transducer $\pm$ 0.3% and air velocity meter $\pm 3.0$ %.

## 3. Mathematical models

*3.1 Model Description*

The $CO_2$ finned-tube gas cooler/condenser can be modelled using two well-known methods: distributed and lumped. The former is a detailed model and has been developed by the authors (Ge and Cropper, 2009), in which the heat exchanger to be modelled is divided into a number of small segments with specified 3-D coordinates i, j and k along directions of pipe length, longitudinal and transverse. For each piece, conservation equations of mass, momentum and energy need to be derived and applied. The detailed model applies localised correlations of heat and mass transfer coefficients and hydraulic processes such that the local

parameter distribution profiles such as temperature, pressure and heat transfer rate, of both hot and cold fluid flowing along the heat exchanger can be accurately predicted. Therefore, the detailed model is believed to be more precise than other modelling methods and is more suitable for analysing and designing complex heat exchangers with intricate pipe circuitry arrangements and uneven air flow distributions. However, if more segments are divided for a modelled heat exchanger, it would require a longer computation time. Therefore it is not entirely appropriate for simulating a refrigeration system where the heat exchanger is integrated with a detailed model. Comparatively, the lumped method is a simple model in which the heat exchanger is divided into very limited number of segments and each is described with conservation equations of mass, momentum and energy. The computation time is thus greatly saved and it is more practical to model a system, although prior model validation with test results is strictly required. The lumped method is therefore used in this paper to model the tested $CO_2$ gas coolers /condensers and the whole system, as shown in Fig. 3, to examine their compatibilities with the system and controls. The comprehensive description of the simple model is given below.

Due to the variations of ambient air temperatures and head pressure controls, the same high-side air cooled heat exchanger in a $CO_2$ refrigeration system can function as either a gas cooler or condenser. It is therefore imperative to model the heat exchanger during both modes of operation. For instance, as seen in Fig. 4, in one pipe circuit the $CO_2$ finned-tube condenser is divided into three segments indicating refrigerant regions of superheated, saturated and subcooled, while the gas cooler has only one section specifying supercritical state. Correspondingly, the fractions of heat transfer areas in those three regions at condenser mode are indicated as $f_{sup}$, $f_{tp}$ and $f_{sub}$ respectively while the $f_{sup}$ for gas cooler mode is set to unity. In addition, there are four pipe rows parallel to the air flow or longitudinal direction, and six pipes in each row or in the transverse direction. It should be noted that for a real heat

exchanger, there are a number of pipe circuits that ensure appropriate refrigerant mass flux and equalised pressure drop through each circuit. As usual, the refrigerant flows from top to bottom, as indicated in the Figure, and the overall heat exchanger flow pattern can be assumed to be cross flow, although other flow designs such as parallel and counter flows may also be modelled using different correlations of the heat transfer.

A simple model at condenser mode can be developed with the following assumptions:

- flow conditions are in a steady state;

- heat conductions along the pipe axis are neglected;

- air flow is distributed homogeneously through each section;

- contact resistance between pipe and fin is ignored;

- refrigerant flow at each cross section is in thermal equilibrium.

For each section of the refrigerant side, the mass conservation is automatically satisfied at the steady state. The momentum equation can be represented by the calculation of pressure drop along the pipe while the energy equations for each section can be calculated as below.

The heat transfer from the refrigerant side is calculated as:

$$\dot{Q} = \dot{m}_r(h_{in} - h_{out}) \tag{1}$$

Where $\dot{m}_r$ is the refrigerant mass flow rate along each section in the same circuit and $h_{in}$ and $h_{out}$ are refrigerant enthalpies at a section inlet and outlet respectively.

Similarly for the air side, the mass balance is automatically fulfilled at the steady state and the pressure drop calculation is also applied for the momentum equation. There is a heat balance between refrigerant and air flows for each section:

$$\dot{Q} = \dot{V}_a \rho_a C_{pa} (T_{aout} - T_{ain})/1000.0 = \varepsilon (G_c)_{min} (T_{rin} - T_{ain}) \tag{2}$$

where the dry coil effectiveness $\varepsilon$ can be calculated as:

$$\varepsilon = \begin{cases} \dfrac{1-\exp(-(1-\exp(-Ntu))(G_c)_{min}/(G_c)_{max})}{(G_c)_{min}/(G_c)_{max}} & \text{for refrigerant in single} - \text{phase} \\ 1 - \exp(-Ntu) & \text{for refrigerant in two} - \text{phase} \end{cases} \tag{3}$$

and,

$$Ntu = \frac{(UA)_{tot}}{(G_c)_{min}} \tag{4}$$

where,

$$(UA)_{tot} = \frac{1}{\frac{1}{(UA)_o} + \frac{1}{(UA)_i}} = \frac{1}{\frac{1}{\eta_f \alpha_o A_o} + \frac{1}{U_i A_i}} \tag{5}$$

For the gas cooler mode, the refrigerant state is always supercritical gas so the above equations applicable for single vapour gas phase can be applied directly. More detailed description and flow chart for the model of condenser with lumped method have been explained and introduced by the authors [16].

The overall heat transfer conductance for 'dry' heat exchangers is calculated by equation (5) and is a function of fin efficiency [17] and heat transfer coefficients from both air and refrigerant sides. For air flow over dry a finned-tube surface, correlations from Wang et. al. are utilized to calculate air-side heat transfer coefficient and pressure drop[18]. At subcritical region, the refrigerant side single phase heat transfer coefficient and pressure drop are

determined using standard turbulent flow relations from the Dittus-Boelter correlation and Blasius equation respectively [19]. For $CO_2$ supercritical gas cooling process, the standard turbulent flow relation is also used for the pressure drop calculation [19], but correlation from Son and Park [20] is applied for the calculation of heat transfer coefficient. Another heat transfer correlation from Dang and Hihara [21] has also been applied with similar simulation results. This is because the air side thermal resistance is much greater than the $CO_2$ side; therefore a small prediction difference on $CO_2$ heat transfer coefficient will not affect the performance of the heat exchanger and its associated system. For the refrigerant two-phase flow, correlations from Dobson and Chato [22], and Müller-Steinhagen and Heck [23] are used to calculate the heat transfer coefficient and pressure drop respectively. To make it clear, more detailed explanation about these correlations were described by the authors [16]. In addition, the refrigerant properties are calculated from the NIST properties software REFPROP 8.

*3.2 Model Validation*

As shown in Fig. 5, two finned-tube $CO_2$ gas coolers/condensers with different sizes and pipe arrangements were investigated experimentally in the refrigeration system described above. The larger one named coil A has 3 rows, 4 pipe circuits, 96 pipes in total and overall dimension 1.6m×0.066m×0.82m (L×D×H) while the smaller one named coil B has 2 rows, 2 circuits, 64 pipes in total and overall dimension 1.6m×0.044m×0.82m (L×D×H). All other structural parameters are the same for both heat exchangers, including a 6.72mm inner diameter of copper pipe, 0.16mm thickness of aluminium fin and 453 fins/m fin density. For these two $CO_2$ heat exchangers, as listed in Table 1, up to 20 tests each were carried out at both the gas cooler and condenser modes and various operating conditions. The table shows

that the gas cooler operates at a higher ambient temperature of up to $35^0$C while the condenser mode tested to a lower ambient air temperature at 19 $^0$C. This imitates real system operations and controls. For both modes and heat exchanger types, the air flow rate varies between 2000 l/s to 2800 l/s, corresponding to 50% to 70% of the full fan speed. From critical points, the refrigerant pressures are controlled up to 90 bar for the gas cooler mode and down to 60 bar for the condenser mode. As such, the refrigerant inlet temperature for the gas cooler mode is much higher than the condenser mode. Simultaneously, the average refrigerant mass flow rates are mostly higher at the gas cooler mode compared to those at the condenser mode.

The detailed model of gas cooler has already been validated [12] and only the simulations with the simple model are compared with the test results of heat releases of the gas cooler and condenser, as shown in Figs. 6 and 7 respectively. Figs. 6 and 7 show that the relative errors of prediction and test results are mostly within ±5% for both the gas cooler and condenser. In addition, the pressure drops of air sides in both the gas cooler and condenser modes are also predicted for those two coils at different operating conditions and compared with corresponding experimental measurements, as shown in Figs. 8 and 9 respectively. The discrepancies of the pressure drop predictions can be seen to be mostly within 15%, which, although acceptable, are not as accurate as those of heat releases. The developed simple model is therefore validated.

As listed in Table 1, the test conditions for both $CO_2$ gas cooler and $CO_2$ condenser are covered which can be used to validate the heat exchanger model at either supercritical or subcritical states. Although the tested $CO_2$ supercritical pressure is up to 90 bar , the validated model can still be used to predict the heat exchanger performance at higher supercritical pressures considering the similar thermosphysical properties and heat transfer behaviours in this region.

## 4.  Model applications

### 4.1 Profiles of refrigerant temperature and local heat transfer rate

As shown in Figs 10 and 11 respectively, a detailed model is used to predict refrigerant temperature and local heat transfer rate profiles along one circuit pipe of the gas cooler for two tested heat exchangers at the specific test conditions listed in Table 2.

The simulation results show that about 90% of the overall temperature drop has taken place in the first 17% of the total circuit pipe length from the inlet.  Similar results can be found from the corresponding measurements, which again demonstrate the accuracy of the detailed model.   This is due to the large temperature difference between the refrigerant and airsides as well as the properties of $CO_2$ in enhancing heat transfer in this region. Similarly, the first row of each gas cooler has the largest heat transfer rate drop, 93.9% for the 3-row and 95.6% for the 2-row coil.   It should be noted that for the heat transfer rate there is a step up when the refrigerant flow turns from one row to the one near to the incoming air flow, such as pipe number 9 for the 3-row coil and pipe number 17 for the 2-row coil. It can be explained that although the refrigerant temperature decreases with an increasing circuit pipe number, the facing air flow temperature for that pipe reduces more due to the pipe row shift. Consequently, the temperature difference increases between refrigerant and air sides for that turning point pipe and thus leads to a higher heat transfer rate.

### 4.2 Effects of heat exchanger sizes and controls

The developed simple $CO_2$ gas cooler/condenser model is then integrated into the existing $CO_2$ booster system to compare and analyse the effects of heat exchanger sizes and controls on the system performance under various design specifications. These include a specified evaporating temperature, superheating, cooling capacity, head pressure controls, approach temperatures and transition ambient temperatures etc., as listed in Table 3. The transition temperature is set to $25\,^0C$ with a 1K dead band , indicating that the system will be in a subcritical cycle if the ambient temperature falls below $24\,^0C$ and transcritical cycle if it rises above $26\,^0C$; otherwise it will remain unchanged. Correspondingly, the floating head pressure control with a 6 K temperature difference and a minimum condensing temperature of $10\,^0C$ is used for the condenser, while the gas cooler pressures can vary from 80 bar to 120 bar. In addition, the heat exchanger fan speeds (or air flow rate) will be modulated to control condenser subcooling to 3K and the gas cooler approach temperature to 2K. For the evaporator in the system, the evaporating temperature and superheating are set to $-5\,^0C$ and 10 K respectively. The cooling capacity is specified to 10 kW and controlled by variable speed of compressors.

For the booster $CO_2$ refrigeration system shown in Fig. 3, a number of Bock $CO_2$ semi-hermetic reciprocating compressors of the same size and type (RKX26/31-4 $CO_2$ T) are to be installed in parallel for the simulation. Based on the manufacture catalogue, the compressor isentropic efficiencies can be correlated and used in the compressor model:

For the compressor in transcritical cycle:

$$\eta_{is} = 0.74443 - 0.050539R_p \tag{6}$$

For the compressor in subcritical cycle:

$$\eta_{is} = 0.6077 - 0.0186R_p \tag{7}$$

As listed in Table 3, at different ambient air temperatures, the cooling capacity is controlled constantly to 10 kW by modulating the motor speed of each operational compressor or a

number of operational compressors. In that case the system cooling COP and the number of operational compressors should be kept the same at a specified ambient air temperature (AAT) and supercritical pressure (gas cooler only) for both $CO_2$ heat exchangers, which are predicted and shown in Figs. 12 and 13 respectively for subcritical and transcritical cycles. As shown in the Figures, for subcritical cycles when the AATs are less than 24 $^0$C, the cooling COP decreases with higher ambient temperatures while the number of operational compressors or compressor power consumptions increase with a warmer ambient. The fraction of the operational compressor number indicates the ratio of motor operational speed to full speed.

For transcritical cycles where the AAT is above 26 $^0$C, the system COP decreases with higher supercritical pressures if the AAT is less than 30 $^0$C but consists of a maximum value if the AAT increases further, leading to an optimal pressure at a specific AAT for a transcritical cycle. Correspondingly, the number of operational compressors increases with higher supercritical pressures when the AAT is between 26 $^0$C and 30 $^0$C but could obtain its lowest value when the temperature is above 30 $^0$C.

On the other hand, for a specific AAT, the refrigerant inlet parameters, including temperature, pressure and mass flow rate, are the same for each heat exchanger although the outlet temperature and pressures will be different. However, the heat exchanger outlet temperature or approach temperature can be controlled by modulating the heat exchanger fan speed or air flow rate, as shown in Figs. 14 and 15 for the condenser and gas cooler respectively. The simulation results show that the air flow rate is always higher for a smaller heat exchanger regardless of whether it acts as a condenser or gas cooler. For the condenser shown in Fig. 14, the air flow rate increases from ambient air temperature (AAT) at 0$^o$C to a top value when the AAT reaches 11$^o$C and then decreases to a minimum when AAT turns to around 19$^o$C and from there goes up to maximum once the AAT is close to a lower transition

point. These results are not expected and therefore need to be further explained . When AAT equals 0°C, the air flow rate is relatively low since at that point the condensing temperature reaches its lowest value and the temperature difference between refrigerant and air is as high as 10 K. When the AAT is above 4 °C, the temperature difference between the condensing temperature and AAT is kept constant at 6 K. Consequently, the condensing temperature increases with a higher AAT and the system requires a greater refrigerant flow rate and thus a higher heat transfer coefficient at tube inside $U_i$ to maintain a constant cooling capacity, but in the meantime the percentage area fraction $f_{tp}$ decreases with a higher AAT. Therefore, the internal UA value and thus the air flow rate of the heat exchanger could increase or decrease with a higher AAT, as seen in Fig. 14. The abrupt increase of air flow rate at 24 °C is due to the great decrease of the inner UA value, considering the very small fraction of $f_{tp}$ exists when the refrigerant is close to the critical point.

For transcritical cycles, as shown in Fig. 15, in most circumstances, at a constant AAT, the air flow rate increases with higher supercritical pressures while at a constant supercritical pressure, the air flow rate increases with a higher AAT. In the meantime, the required air flow rate is higher for a smaller gas cooler. For the 2-row gas cooler, when AAT is higher than 35 ⁰C, it reaches its lowest air flow rate.  This is the reason that there exists an optimal COP or minimum power consumption and thus lower refrigerant mass flow rate and therefore the refrigerant is easier to be cooled down.   In addition, if the approach temperature is not controlled, the model can predict how far that the approach temperature could be reduced when the gas cooler air flow rate increases gradually, as show in Figure 16 for the 3-row heat exchanger.  It is seen that at the same refrigerant inlet condition and ambient temperature, a great decrease in the refrigerant outlet temperature or approach temperature of the gas cooler can be predicted when air flow rate increases from 500 l/s to 1000 l/s.  When the air flow rate increases father, the approach temperature will carry on decreasing but with a reduced rate. In the meantime, the simulation results also show that at a constant air flow rate, the approach temperature increases with higher $CO_2$ pressure.   The simulation results can further demonstrate the effect of air flow rate on the approach temperature at the gas cooler outlet and eventually the system performance.

**5. Conclusions**

In varying ambient air temperatures, the high pressure $CO_2$ heat exchanger in a $CO_2$ refrigeration system will operate as either a gas cooler or condenser. The heat exchanger needs to be well designed and controlled so as to maximize the performance of its integrated system.  Accordingly, two different sized and structural $CO_2$ fined-tube heat exchangers are

manufactured and installed in a test rig of a $CO_2$ booster system. Extensive experiments have been carried out in the test rig at different operating states and controls. In the meantime, the $CO_2$ heat exchanger models have been developed using two methods : distributed and lumped. The former needs to be utilised if detailed profiles of temperature and heat transfer rate along a pipe circuit are required. However, the latter method is suitable for a system simulation when the heat exchanger model is integrated into an overall system. The models have been validated with corresponding experiment measurements and are thereafter used to predict the effects of the heat exchanger sizes and controls on the system performance.

The simulation results show that around 90% of the overall temperature drop occurs in the first 17% of the total circuit pipe length from the inlet. Moreover, over 90% of the total heat transfer rate drop happens in the first row of each heat exchanger. In addition, the system cooling COP decreases with higher ambient air temperatures for both subcritical and transcritical cycles but for a transcritical cycle, there is an optimum supercritical pressure when the ambient air temperature is higher. Furthermore, the fan speed controls can be utilised to modulate and control the subcooling and approach temperature for the condenser and gas cooler respectively at a fixed subcritical or supercritical pressure. However, a higher fan speed is required if the heat exchanger size is reduced. In addition, the simulation results show further that the variation of air flow rate is the most effective way to control and minimise the approach temperature of the gas cooler although the decrease rate is significant reduced if the air flow rate is much higher.

**References**

[1]  Schiesaro P, Kruse H. Development of a two stage $CO_2$ supermarket system, IIF-IIR, New technologies in commercial refrigeration 2002; Urbana, Illinois, USA.

[2] Getu HM, Bansal PK, Thermodynamic analysis of an R744–R717 cascade refrigeration system. International Journal of Refrigeration 2008 ;31: 45–54.

[3] Bhattacharyya S, Mukhopadhyay S, Kumar A, Khurana RK, Sarkar J,  Optimization of a CO2–$C3H_8$ cascade system for refrigeration and heating. International Journal of Refrigeration  2005; 28 : 1284–1292.

[4]  Kim MH, Pettersen J, Bullard CW. Fundamental process and system design issues in $CO_2$ vapor compression systems. Progress in Energy and Combustion Science 2004; 30:119-174.

[5]  Ge YT, Tassou SA. Control optimisation of $CO_2$ cycles for medium  temperature retail food refrigeration systems. International Journal of Refrigeration 2009 ; 3 2 :  1 3 7 6 – 1 3 8 8.

[6]  Cavallini A., Cecchinato L., Corradi M., Fornasieri E., Zilio C.
    Two-stage transcritical carbon dioxide cycle optimisation: A theoretical and
    experimental analysis. International Journal of Refrigeration 2005; 28 : 1274–1283

[7]  Hwang Y., Jin DDH., Radermacher  R., Hutchins JW.  Performance measurement of
    $CO_2$ heat exchangers, ASHRAE Transactions 2005; 306–316.

[8]   Srinivas SP., Groll EA.,  Ramadhyani S. New correlation to predict the heat transfer coefficient during in-tube cooling of turbulent supercritical $CO_2$. International Journal of Refrigeration 2002; 25 : 887–895.

[9]   Yoon SH., Kim JH.,  Hwang YW., Kim MS., Min K., Kim Y. Heat transfer and pressure drop characteristics during the in-tube cooling process of carbon dioxide in the supercritical region. International Journal of Refrigeration 2003; 26:857–864.

[10]   Son CH.,  Park SJ. An experimental study on heat transfer and pressure drop characteristics of carbon dioxide during gas cooling process in a horizontal tube. International Journal of Refrigeration 2006; 29:539–546.

[11]   Ge YT, Cropper R. 2008, Performance simulation of refrigerated display cabinets operating with refrigerants R22 and R404A. Applied Energy, V85(8):694-707.

[12]   Ge YT, Cropper R. Simulation and performance evaluation of finned-tube $CO_2$ gas coolers for refrigeration systems. Applied Thermal Engineering 2009; 29: 957-965.

[13]  Lin KH, Kuo CS,  Hsieh WD, Wang CC, Modeling and simulation of the transcritical CO2 heat pump system. International Journal of Refrigeration 2013; 36:2048-2064.

[14]  Yang JL, Ma YT, Li MX, Hua J, Modeling and simulating the transcritical CO2 heat pump system. Energy 2010; 35:4812-4818.

[15]   Chang YS, Kim MS. Modelling and performance simulation of a gas cooler for  $CO_2$ heat pump system. HVAC&R Research 2007 ; 13: 445-456.

[16]  Ge YT, Cropper R. Performance evaluations of air-cooled condensers using pure and mixture refrigerants by four-section lumped modelling methods. Applied Thermal Engineering 2005; 25:1549–1564.

[17]   Incropera FP, DeWitt DP. Introduction to Heat Transfer, third ed., John Wiley and Sons 1996; New York.

[18] Wang CC, Lee WS, Sheu WJ. A comparative study of compact enhanced finand-tube heat exchangers, International Journal of Heat Mass Transfer 2001; 44 : 3565–3573.

[19] Incoprera FP, De Witt DP. Fundamentals of heat and mass transfer. New York: John Wiley; 1990.

[20] Son CH, Park SJ. An experimental study on heat transfer and pressure drop characteristics of carbon dioxide during gas cooling process in a horizontal tube . International Journal of Refrigeration 2006 ;29: 539–546

[21] Dang C, Hihara E. In-tube cooling heat transfer of supercritical carbon dioxide. Part 1. Experimental measurement. International Journal of Refrigeration 2004:27(7): 736-747.

[22]  Dobson MK, Chato JC. Condensation in smooth horizontal tubes. J Heat Trans Trans ASME 1998; 120:193–213.

[23]  Muller-Steinhagen H., Heck K. A simple friction pressure-drop correlation for two-phase flow in pipes. Chem Eng Process 1986; 20:297–308.
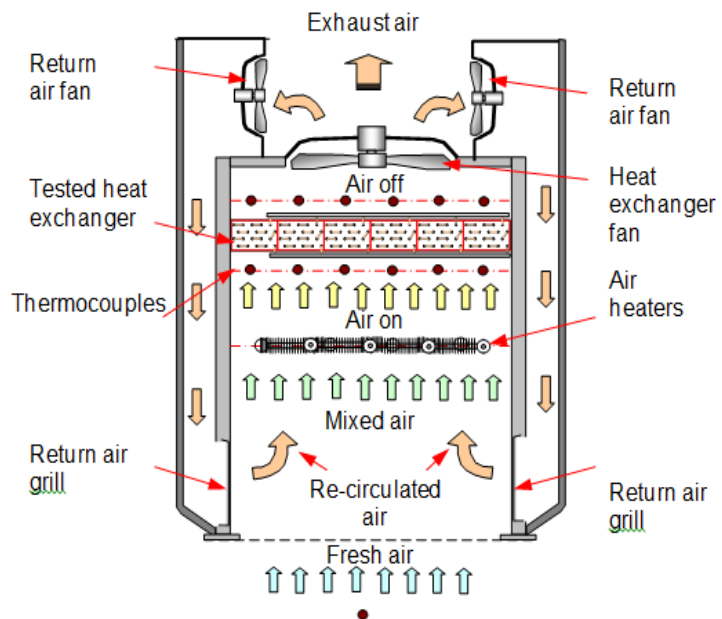
**Fig. 1.** Test rig of $CO_2$ gas cooler & condenser

**Ref. in**

**Ref. out**
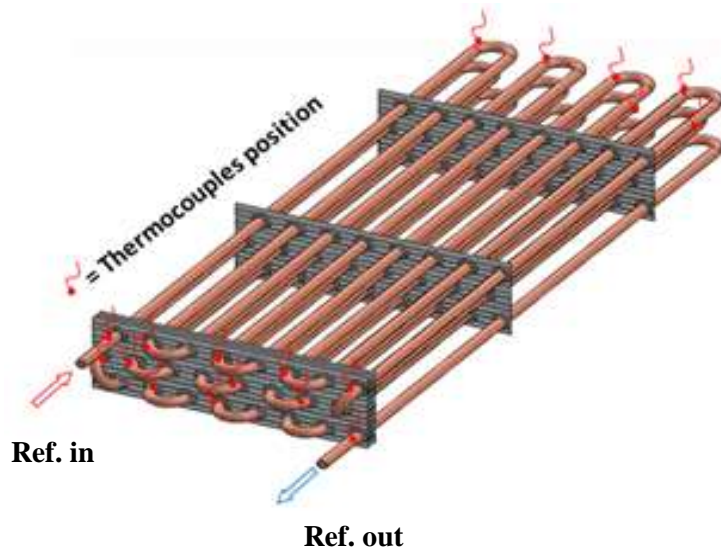
**Fig. 2.** Pipe arrangement and   locations in one heat exchanger circuit
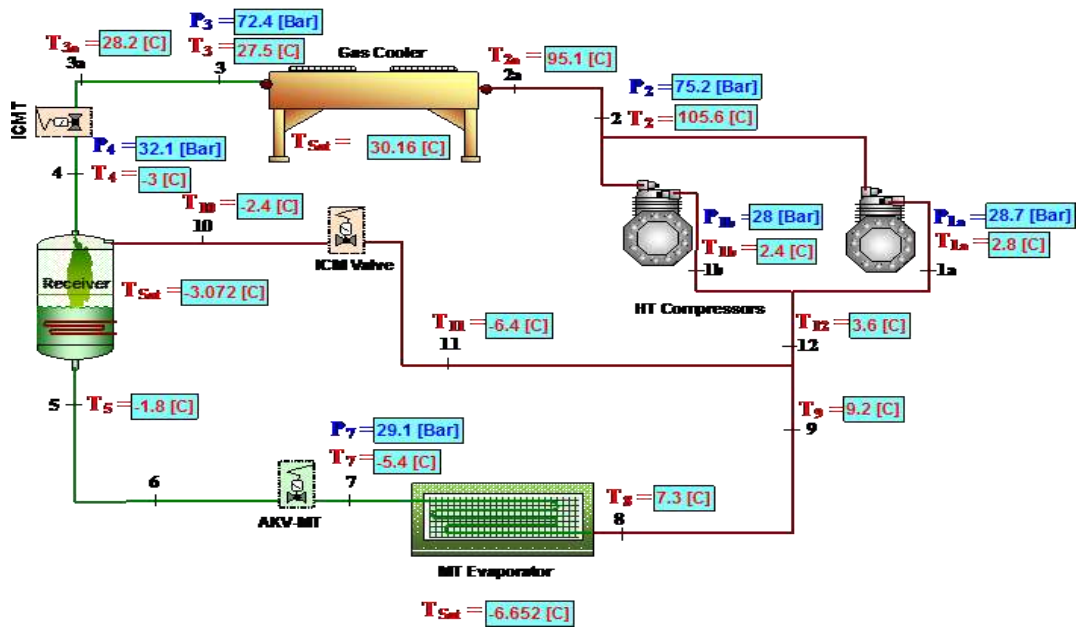
**Fig. 3.** Tested $CO_2$ gas cooler/condenser and its integrated refrigeration system
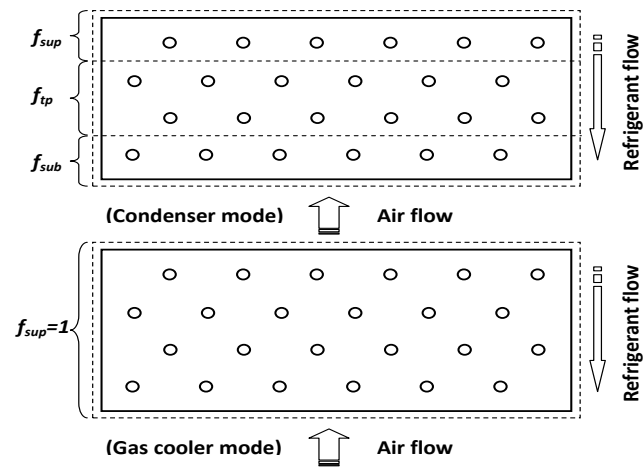
**Fig. 4.** Single circuit heat exchanger and segment divisions at condenser and gas cooler modes
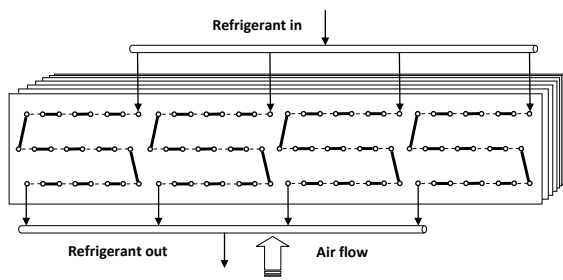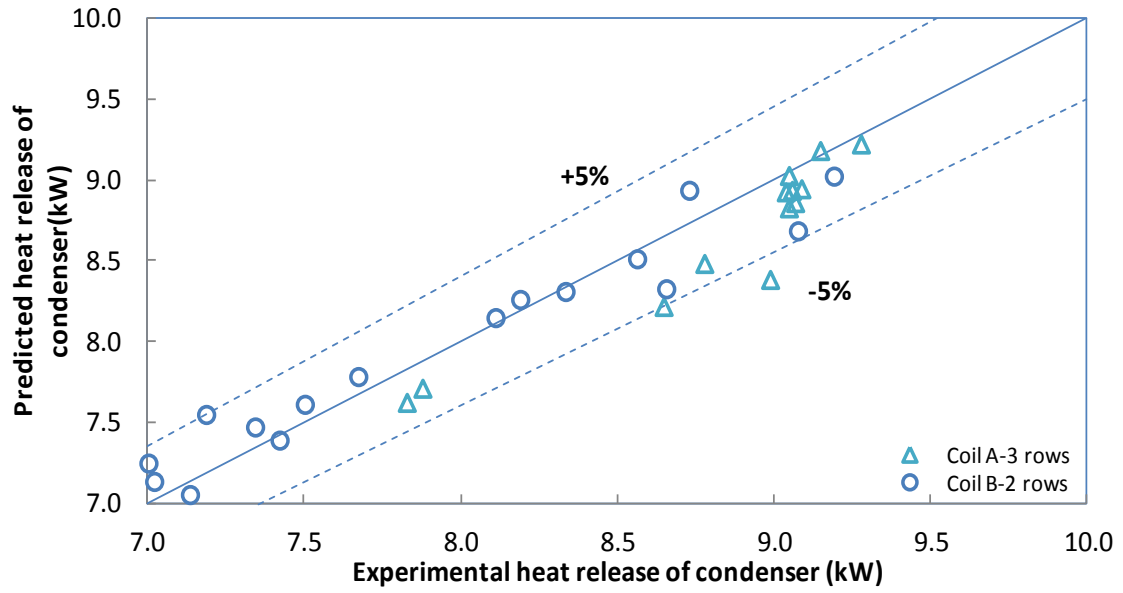
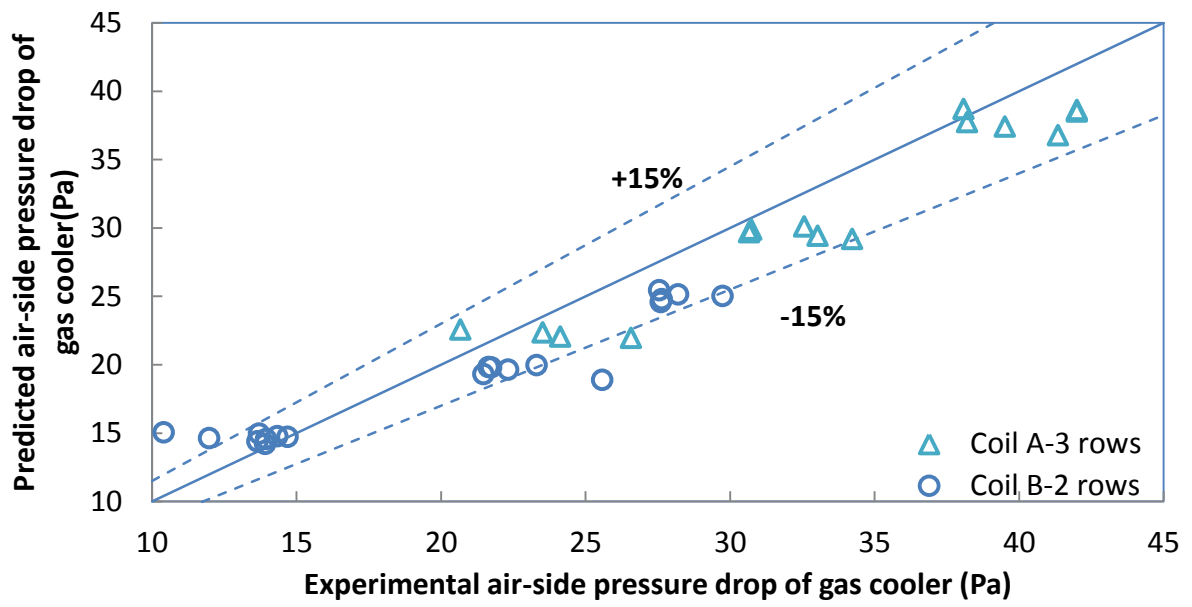(Coil A-3 rows 4 circuits)  (Coil B-2 rows 2 circuits)
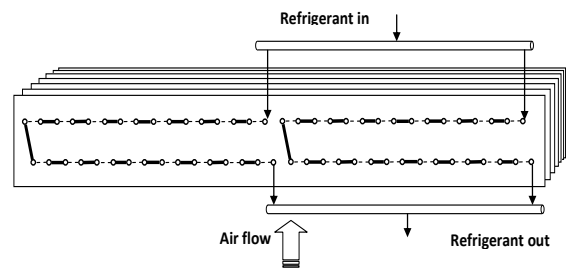
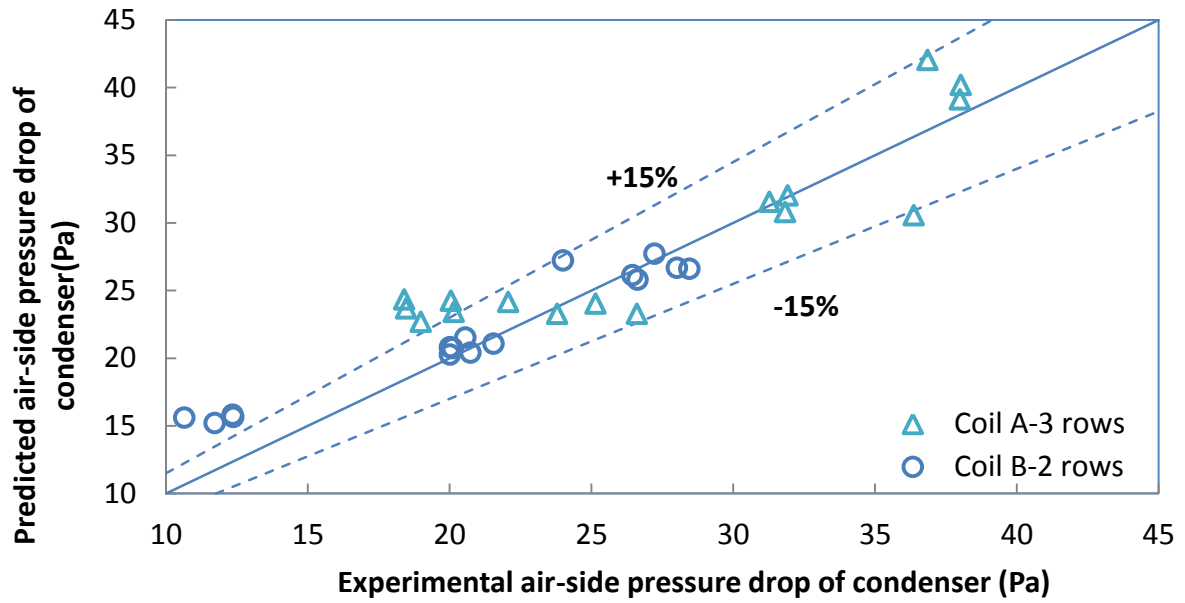**Fig. 5.** two tested finned-tube $CO_2$ gas coolers/condensers
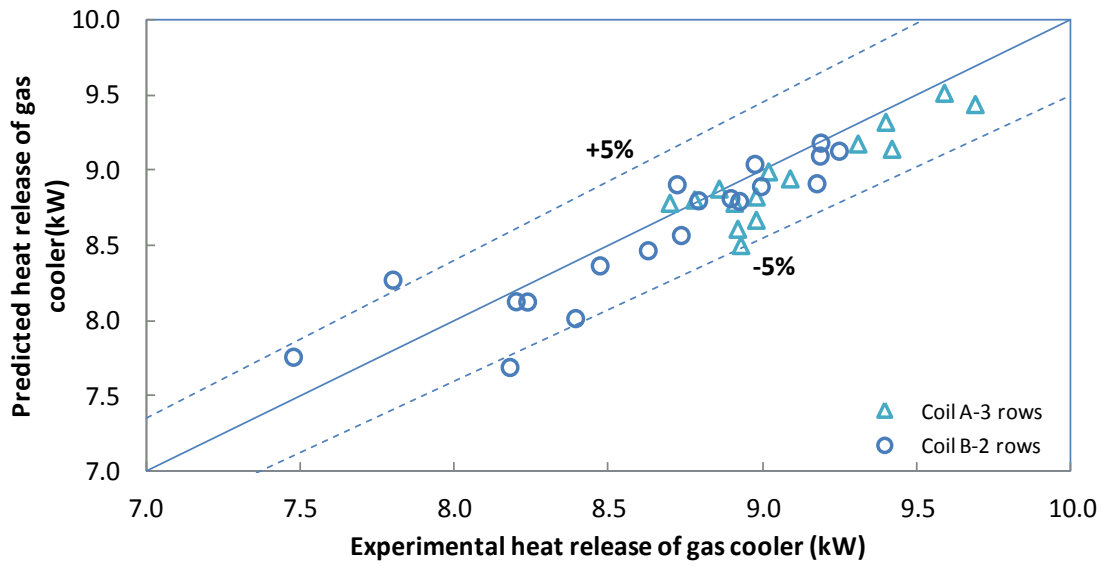
**Fig. 6.** Comparison of simulation and experimental results for heat release of gas cooler

**Fig. 7.** Comparison of simulation and experimental results for heat release of condenser

**Fig. 8.** Comparison of simulation and experimental results for air side pressure drops of gas coolers

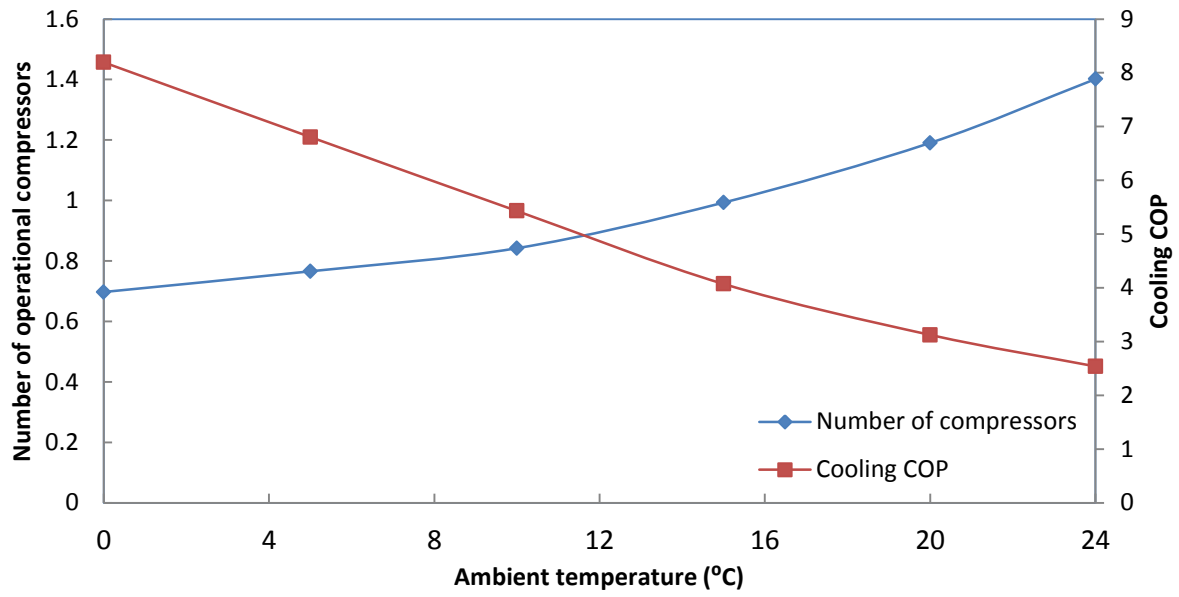**Fig. 9.** Comparison of simulation and experimental results for air side pressure drops of condensers
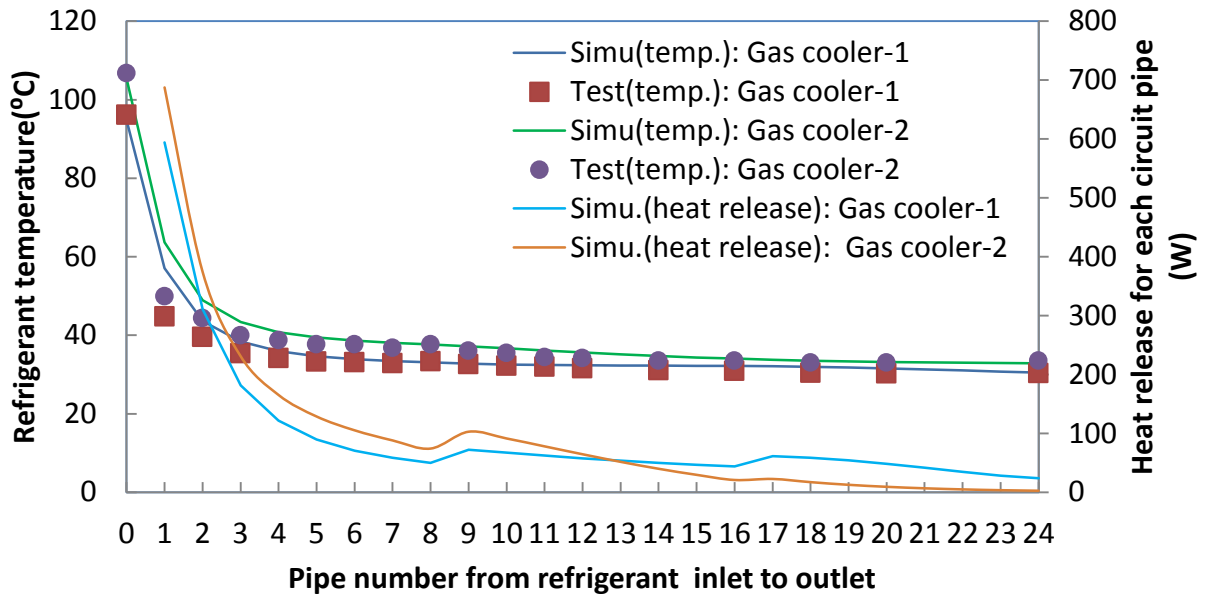
**Fig. 10.** Profiles of temperature and heat transfer rate along the pipes of each circuit for the 3-row gas cooler.
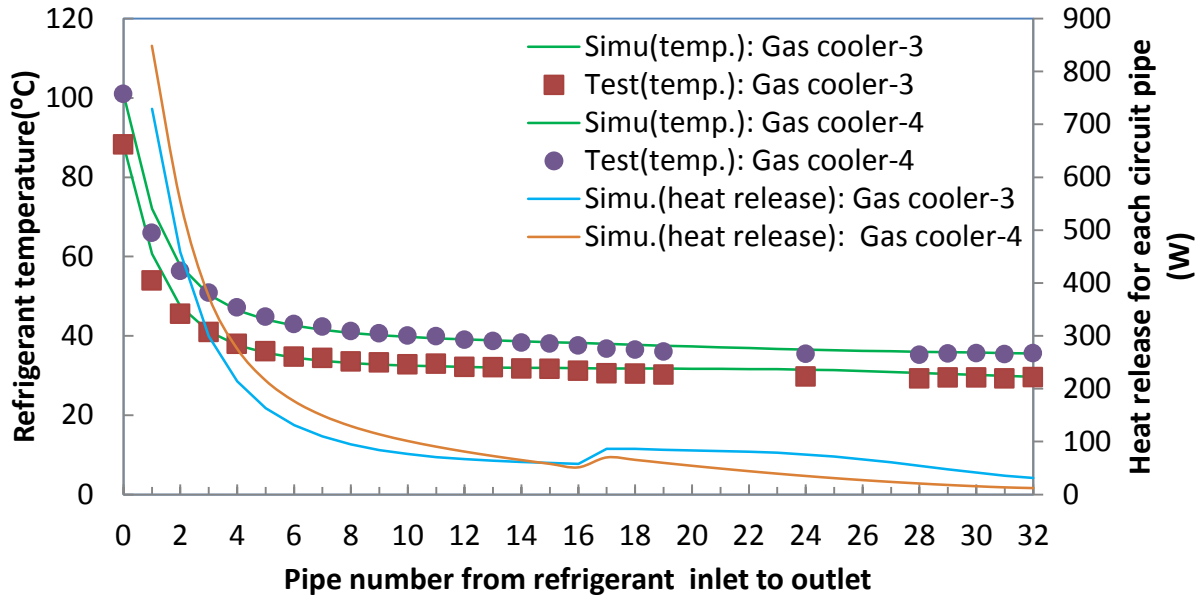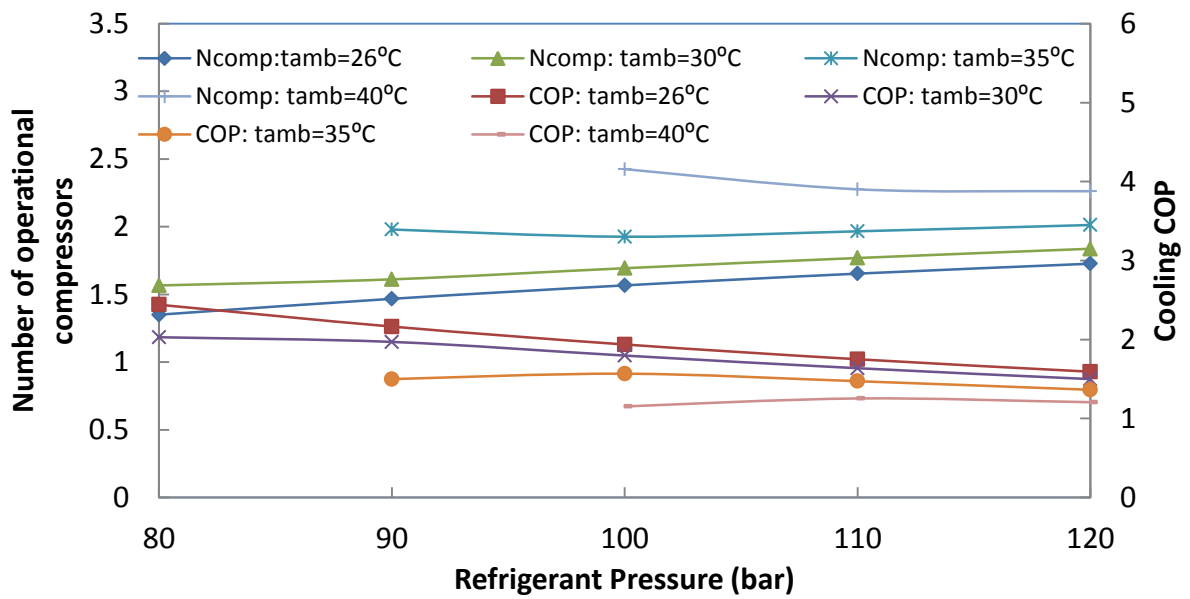
**Fig. 11.** profiles of temperature and heat transfer rate along the pipes of each circuit for the 2-row gas cooler.
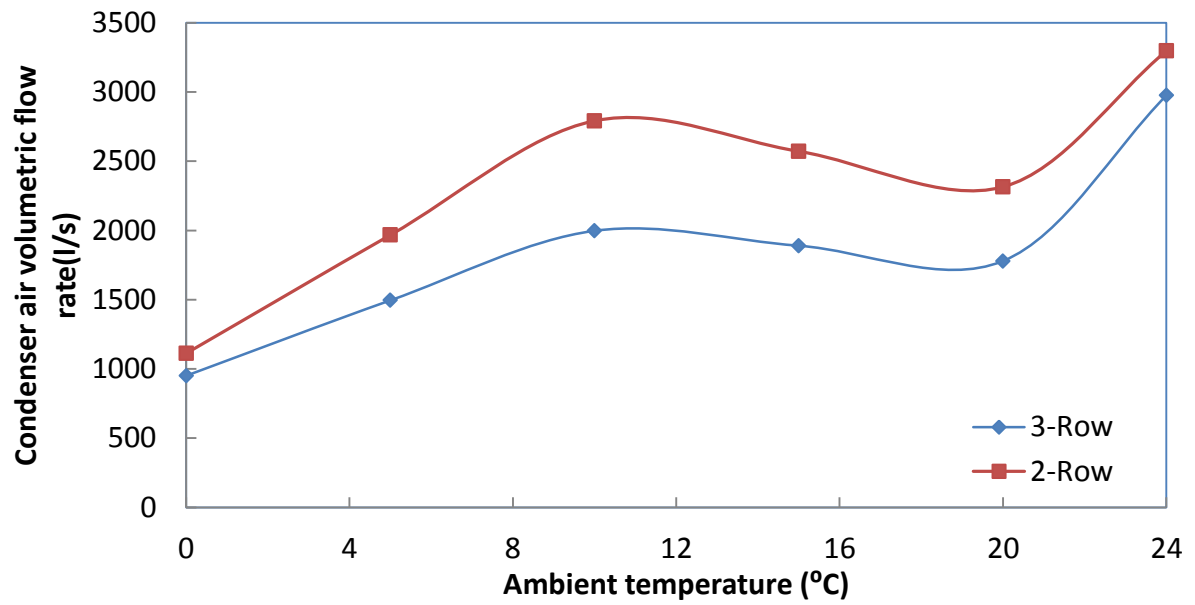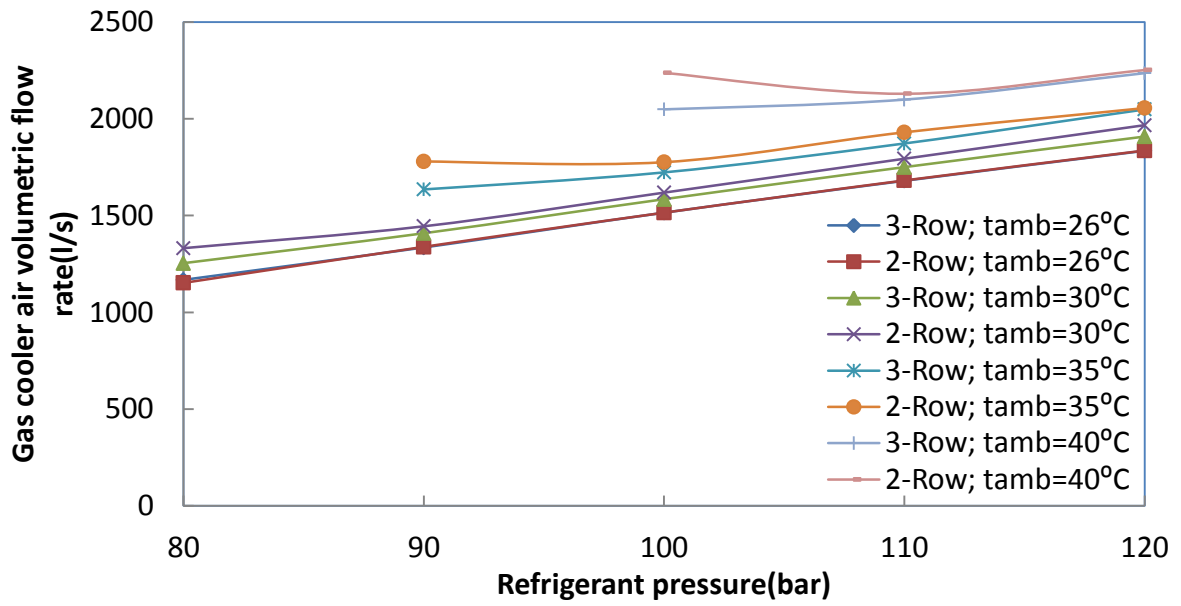
**Fig. 12.** Variation of number of operational compressors and cooling COP in the system with ambient temperature

**Fig. 13.** Variation of number of operational compressors and cooling COP in the system with

$CO_2$ supercritical pressure and ambient air temperature

**Fig. 14.** Variation of volumetric flow rate with ambient temperature for different $CO_2$ condensers

**Fig. 15.** Variation of volumetric flow rate with supercritical pressure and ambient air temperature for different $CO_2$ gas cooler
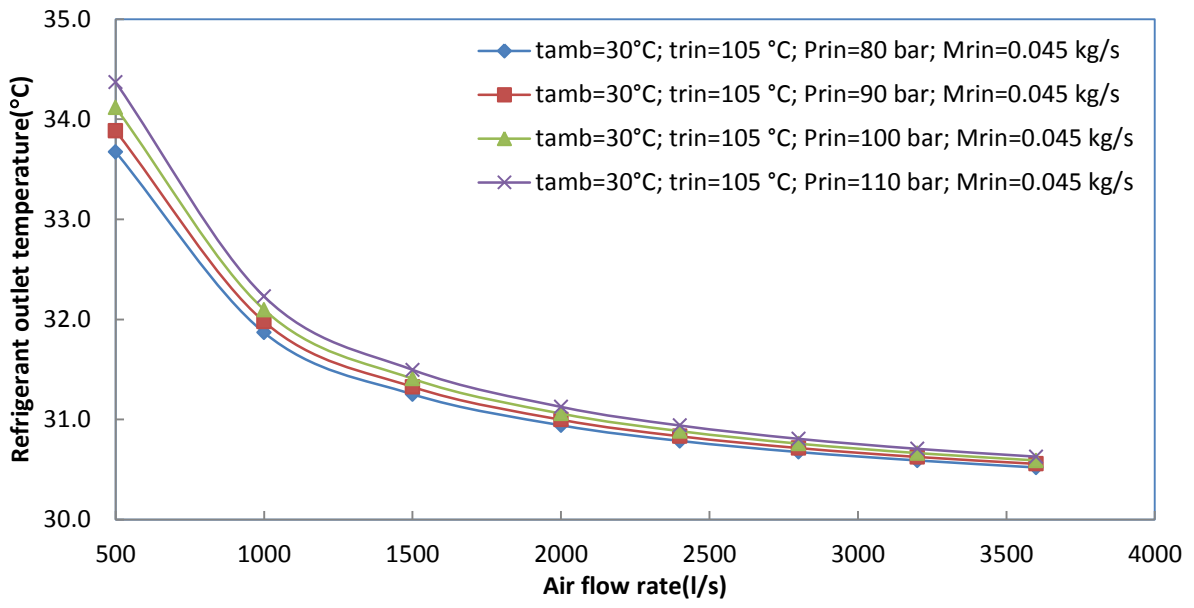
**Fig. 16.** Variation of refrigerant temperature at the gas cooler (3-row) outlet air flow rate

**Table 1.** Test conditions of $CO_2$ heat exchangers for both gas cooler and condenser modes

| Mode | HX Type | No. of Tests | Test ranges | | | | |
|---|---|---|---|---|---|---|---|
| | | | $T_{ain}$ | $\dot{V}_a$ | $T_{rin}$ | $P_{rin}$ | $\dot{m}_r$ |
| | | | $^0C$ | l/s | $^0C$ | bar | kg/s |
| Gas cooler | 3 Rows | 15 | 28~35 | 2000~2800 | 90~120 | 75~90 | 0.036~0.042 |
| | 2 Rows | 19 | 28~35 | 2000~2800 | 90~120 | 75~90 | 0.036~0.042 |
| Condenser | 3 Rows | 16 | 19~29 | 2000~2800 | 71~90 | 60~73 | 0.031~0.040 |
| | 2 Rows | 17 | 19~29 | 2000~2800 | 71~90 | 60~73 | 0.031~0.040 |

**Table 2.** Specific test conditions of $CO_2$ gas coolers for validation and application of detailed

model

| Mode | HX Type | Test ranges | | | | |
| --- | --- | --- | --- | --- | --- | --- |
| | | $T_{air\_on}$ | $\dot{m}_{aflow}$ | $T_{rin}$ | $P_{rin}$ | $\dot{m}_{rin}$ |
| | | $^0C$ | l/s | $^0C$ | bar | kg/s |
| Gas cooler-1 | 3 rows | 29.54 | 2000 | 94.93 | 76 | 0.041 |
| Gas cooler-2 | 3 rows | 32.77 | 2000 | 105.54 | 85.14 | 0.042 |
| Gas cooler-3 | 2 rows | 28.46 | 2000 | 88.11 | 75.37 | 0.035 |
| Gas cooler-4 | 2 rows | 35.14 | 2000 | 100.85 | 87.27 | 0.038 |

**Table 3** Specification of system component parameters and controls

| Component | Parameter | Control |
|---|---|---|
| Evaporator | Evaporating temperature | $-5^0$C |
| | Superheating | 10K |
| | Cooling capacity | 10 kW |
| Compressor | Cooling capacity | Variable speed |
| Gas cooler /Condenser | Supercritical pressure | Constant 80~120 bar |
| | Subcritical pressure | Floating Dt=6K |
| | Minimum condensing temperature | $10^0$C |
| | Gas cooler approach temperature | 2K with Fan Speed |
| | Condenser subcooling | 3K with Fan Speed |
| Vessel | Pressure | 32.164 bar ($-5^0$C Sat) |
| Transcritical-Subcritical Cycle | Transition ambient temperature | $25\pm1^0$C |